Annals of Nuclear Energy 195 (2024) 110194

Contents lists available at ScienceDirect

Annals of Nuclear Energy

journal homepage: www.elsevier.com/locate/anucene

Assessment of cladding ballooning during DBA-LOCAs with FRAPTRAN

F. Feria *, P. Aragón, L.E. Herranz

Unit of Nuclear Safety Research, CIEMAT, Avda. Complutense 40, 28040 Madrid, Spain

ARTICLE INFO

Keywords:
Cladding ballooning
LOCA
Modelling
Fuel safety

ABSTRACT

The assessment of cladding degradation mechanisms under anticipated DBA LOCA conditions requires analytical tools capable of properly modelling the processes involved in clad deformation and burst. The present work proves that the deviations found in FRAPTRAN simulations of burst and LOCA tests, mostly concerning time to failure, come to a good extent from the high temperature creep law, whereas failure limits barely play any role in the deviations. According to an analysis conducted with an alternative model, one might conclude that a Norton-type formulation, once extended to irradiated conditions, might substantially enhance FRAPTRAN accuracy. Besides, this work shows how the formulation adopted to estimate plastic strains up to the instability strain also plays an important role in the time-to-failure prediction.

1. Introduction

An accurate knowledge of the fuel rod performance under design basis accidents (DBA) is of utmost importance for safety reasons, mainly focused on preserving the cladding integrity and the core coolability (USNRC, 2021). Because of that, the understanding of the cladding mechanical performance and its failure modes are key aspects in fuel safety assessments in DBAs.

Under DBA LOCA (loss of coolant accident) conditions in LWR (Light Water Reactors), the fuel rod heating up may give rise to cladding ballooning due to the high temperatures attained at local hot spots (Meyer and Wiesenack, 2022). This phenomenon implies fast and significant local viscoplastic deformation of the cladding that can lead to coolant mass flow reduction between rods and, more importantly, to cladding burst and the subsequent release of fission products. It is shown that ballooning fosters fuel fragmentation, relocation and dispersal upon bursting (FFRD), being the phenomenon of FFRD especially important at high burnup (from a pellet average burnup of roughly 60 GWd/tU) (Wiesenack, 2013; Wiesenack, 2015; OECD/NEA, 2016).

In this context, fuel performance codes play a key role to predict the cladding mechanical behavior under the anticipated LOCA conditions. The analytical capabilities developed to do that are submitted to continuous verification, validation and improvement (IAEA, 2012; IAEA, 2013; IAEA, 2019; IAEA, 2020). Particularly, changes in fuel design, new cladding materials, more challenging operating conditions and the trend towards higher burnups, emphasize the need to check the validity of fuel performance codes. In that regard, FUMAC (FUel Modeling in Accident Conditions) has been a recent coordinated research project of the IAEA targeted specifically to assess the capability of fuel performance codes to LOCA conditions, based on experimental data coming from several laboratories (Halden, Studsvik, MTA-EK and QUENCH) (IAEA, 2019).

FUMAC concluded that, despite the enhancement achieved so far on clad ballooning, it still requires further improvement (IAEA, 2019). In the particular case of the widely used code FRAPTRAN (Geelhood et al., 2016), an important uncertainty in the mechanical behavior prediction was found, although it was not considered fully responsible for the deviation noted with respect to time-to-failure data measured (IAEA, 2019; Peláez and Herranz, 2017). However, the intrinsic uncertainties of the code's ballooning model (i.e., bias of high temperature creep law and failure limits) were not taken into account. Therefore, further analysis would be needed to fully understand the code's deviations in key variables like cladding deformation and time to failure, if burst happens.

The main objective of this work is to assess and improve the FRAPTRAN's mechanical model capabilities for predicting the cladding integrity under LOCA conditions that imply large deformation (i.e., burst due to ballooning). To do that, the code has been extended with the bias of the high temperature creep model and the failure limits. Additionally, an alternative high temperature creep law has been implemented to further analyse the impact of the viscoplasticity modelling. The validation database used comes from separated effect tests and integral tests considered in the FUMAC project; particularly, selected cases from the PUZRY series (burst tests) and IFA-650 tests from the Halden research reactor have been simulated.

* Corresponding author.
E-mail address: francisco.feria@ciemat.es (F. Feria).

https://doi.org/10.1016/j.anucene.2023.110194
Received 14 June 2023; Received in revised form 27 September 2023; Accepted 14 October 2023
Available online 18 October 2023

2. Mechanical modelling

2.1. Overview

The FRAPTRAN code is a transient fuel performance predictive tool developed by PNNL to be applied to design basis accident conditions (RIA, LOCA) (Geelhood at al., 2016). It uses the FRACAS-I model to predict the mechanical response of fuel and cladding for small strains and the BALON2 model to predict clad ballooning (i.e., large strains). As it will be shown, both models are fed with MATPRO's correlations for Zirconium-based alloys claddings (USNRC, 2001).

Fig. 1 depicts how the mechanical modelling of FRAPTRAN works. At the end of each load increment calculation, the cladding effective plastic strain, ^{ep}, is obtained by FRACAS-I and compared to the instability strain, $^{ep}_{inst}$ (a value of 5 % is imposed). If the calculated strain does not reach the instability strain, a new load is calculated by FRACAS-I model. However, if the calculated strain is greater than this limit, it is assumed that ballooning occurs (large localized non-uniform deformation) at that axial node. Then, the BALON2 model is used by FRAPTRAN. In this case, FRACAS-I is no longer used for cladding (the corresponding calculations stop in all the nodes), and BALON2 performs strain calculations only for the ballooning node. BALON2 predicts cladding failure if the true hoop stress is greater than an empirical stress limit or if cladding plastic hoop strain is greater than an empirical strain limit (Fig. 2).

The following sections shows the details of the mechanical modelling of FRAPTRAN with the focus on the cladding plastic deformation up to failure, as one of the main targets under LOCA conditions.

2.2. FRACAS-I

The cladding deformation model in FRACAS-I is based on the incremental theory of plasticity, applied in each axial node. Neither circumferential nor radial nodalization of the cladding is considered in the modelling according to the axisymmetry approach and the thin-shell theory, respectively. Note that axisymmetry only yields an approximate solution since actual cases are not axisymmetric (Karb et al., 1983; Stuckert et al., 2020).

The relationship between the components of the plastic strain increments, $d\varepsilon_i^p$ (i: hoop, θ, axial, z, radial, r), and the effective plastic strain increment, $d\varepsilon^p$, is provided by the Prandtl-Reuss isotropic flow rule:

$$d\varepsilon_i^p = \frac{3}{2}\frac{d\varepsilon^p}{\sigma_{eff}}\left[\sigma_i - \frac{1}{3}(\sigma_\theta + \sigma_z + \sigma_r)\right] \tag{1}$$

where σ_i are the cladding stress components and σ_{eff} is the effective von Mises stress. Additionally, the condition of incompressibility is fulfilled:

$$d\varepsilon_\theta^p + d\varepsilon_z^p + d\varepsilon_r^p = 0 \tag{2}$$

The cladding stress components are calculated based on the pressure difference between the fuel side (rod internal pressure, P_i, assuming no pellet-clad mechanical contact under LOCA conditions) and the coolant side (external pressure, P_o):

$$\begin{aligned}\sigma_\theta &= \frac{r_i P_i - r_o P_o}{r_o - r_i}\\ \sigma_z &= \frac{r_i^2 P_i - r_o^2 P_o}{r_o^2 - r_i^2}\end{aligned} \tag{3}$$

with r_i and r_o the uniform inner and outer cladding radius, respectively. Note that the radial stress, σ_r, is assumed to be negligible according to the approach carried out by the code (i.e., thin shell theory). Based on the stress components, the cladding effective stress is calculated as:

$$\sigma_{eff} = \sqrt{\frac{(\sigma_\theta - \sigma_z)^2 + (\sigma_z - \sigma_r)^2 + (\sigma_r - \sigma_\theta)^2}{2}} \tag{4}$$

The effective plastic strain increment is determined from the basic MATPRO's equation that relates stress and plastic strain:

$$\sigma_{eff} = K\cdot(\varepsilon^p)^n\cdot\dot{\varepsilon}^m \tag{5}$$

where K is the strength coefficient, n the strain hardening exponent and m the strain rate exponent, being $\dot{\varepsilon}$ the strain rate. These coefficients depend on temperature, fast neutron fluence and material cold work. The two latter are related to the corresponding hardening effect, although both fast neutron fluence and material cold work are also correlated with the temperature to simulate the hardening recovery under high temperature conditions (annealing). The details of these parameters are reported elsewhere (USNRC, 2001; Geelhood et al., 2008).

2.3. BALON2

As previously mentioned, the BALON2 model calculates the non-uniform large cladding deformation that occurs between the time that the cladding plastic strain exceeds the instability strain and the time of cladding rupture, if it happens. The model divides the ballooning axial node into circumferential and axial subnodes, as shown in Fig. 3. The cladding is assumed to consist of a network of membrane elements subjected to a pressure difference between the inside surface and the outside surface.

The plastic strain increment components are determined by the Prandtl-Reuss flow rule taking into account the anisotropies of the cladding material according to MATPRO's formulation (USNRC, 2001):

$$\begin{aligned}d\varepsilon_\theta^p &= \frac{d\varepsilon^p\cdot[a\cdot(\sigma_\theta - \sigma_z) + b\cdot(\sigma_\theta - \sigma_r)]}{\sigma_{eff}}\\ d\varepsilon_z^p &= \frac{d\varepsilon^p\cdot[c\cdot(\sigma_z - \sigma_r) + a\cdot(\sigma_z - \sigma_\theta)]}{\sigma_{eff}}\\ d\varepsilon_r^p &= \frac{d\varepsilon^p\cdot[b\cdot(\sigma_r - \sigma_\theta) + c\cdot(\sigma_r - \sigma_z)]}{\sigma_{eff}}\end{aligned} \tag{6}$$

with a, b and c anisotropy coefficients. The condition of incompressibility is not applied in this model. The stress and strain are calculated with the basis shown in the previous section but taking into account the non-uniform shape of the cladding at ballooning (Hagrman, 1981). Particularly, radial and hoop stress are estimated as follows:

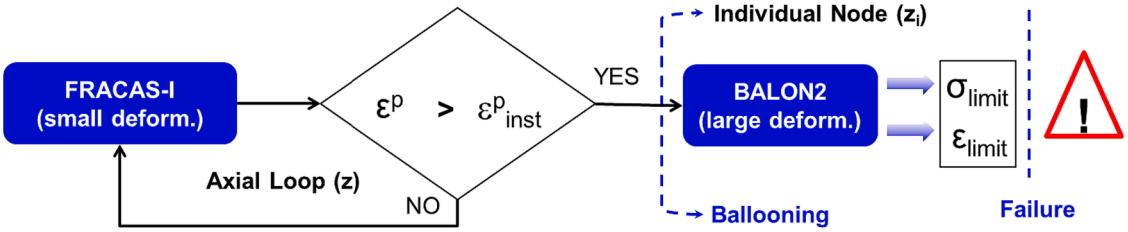

Fig. 1. Scheme for the FRATRAN's mechanical modelling.

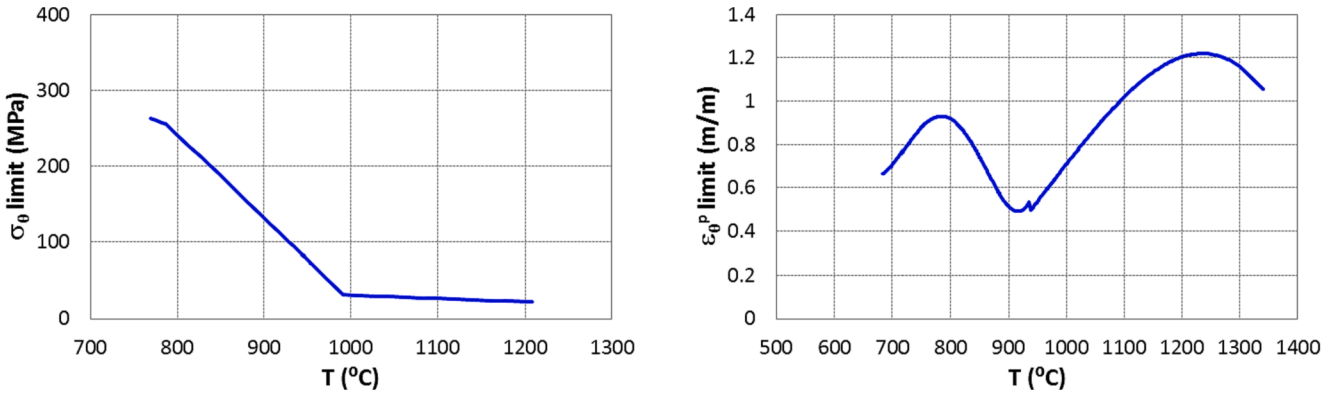

Fig. 2. BALON2 empirical limits: true hoop stress limit (Figure on the left) and plastic hoop strain limit (Figure on the right).

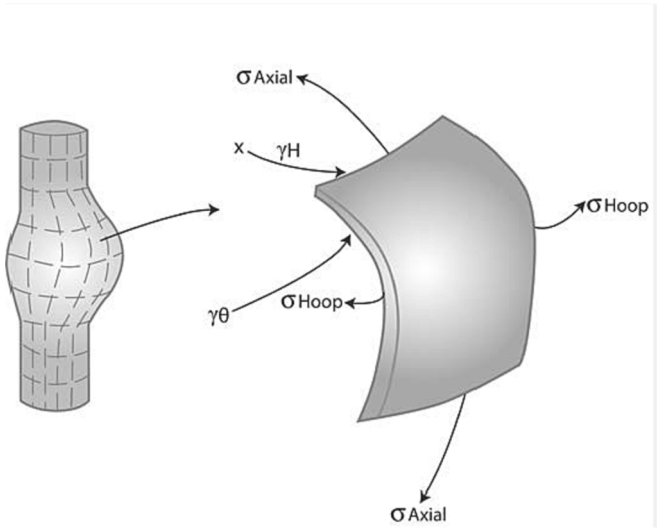

Fig. 3. Scheme for the BALON2 nodalization (Geelhood at al., 2016).

$$\sigma_r = -\frac{r_i P_i + r_o P_o}{r_o + r_i} \tag{7}$$

$$\sigma_\theta = \frac{r_i P_i - r_o P_o}{r_o - r_i} - \frac{(P_i - P_o)(\delta - (r_o - r_i))\cdot r_{av}}{(r_o - r_i)^2} + \frac{r_{av}\cdot\sigma_z}{[\exp(\varepsilon_z)]^2}\frac{\partial^2 r_{av}}{\partial z^2} \tag{8}$$

with r_i and r_o the non-uniform inner and outer cladding radius, δ the local thickness (non-uniform due to the ballooning shape), r_{av} the midwall radius and ε_z the total axial strain.

In order to obtain the effective plastic strain increment according to the mechanical behavior anticipated in the ballooning zone (i.e., high-temperature creep strain), the BALON2 model uses the following equation from MATPRO (USNRC, 2001):

$$\varepsilon^p = \left[\left(\frac{n}{m}+1\right)10^{-3}\left(\frac{\sigma_{eff}}{K}\right)^{1/m} dt + \varepsilon_{i-1}^{\left(\frac{n}{m}+1\right)}\right]^{\frac{m}{m+n}} \tag{9}$$

This equation yields the true effective strain at the end of a time interval. It is based on the same concept as Eq. (5), using the coefficients K, n, and m, previously mentioned. In other words, the formulation used in BALON2 model to estimate viscoplasticity is based on parameters fitted to stress–strain curves. Note that FRAPTRAN has the option to use Eq. (9) instead of Eq. (5) in FRACAS-I; indeed, it is the option selected by default in the code during the open gap regime.

According to the review carried out, the mechanical approach used in a fuel performance code like FRAPTRAN to predict the cladding mechanical performance under ballooning regime is consistent. However, when it comes to the formulation used to determine the cladding viscoplastic behavior, alternative modelling should be explored.

3. Modelling adaptation

In order to explore alternative creep modelling, a Norton law commonly used in other fuel performance codes has been implemented in FRAPTRAN as an option. Additionally, the bias of both creep models (i.e., default and Norton) and the bias of the failure limits have also been implemented to check the corresponding uncertainty in the predictions made. The following sections show the details of the adaptations carried out.

3.1. Alternative creep law

The Norton creep law is applied in fuel performance codes like TRANSURANUS (Di Marcello et al., 2014) or BISON (Pastore et al., 2021). It is formulated as follows:

$$d\varepsilon^p = A\cdot\exp\left(-\frac{Q}{R\cdot T}\right)\cdot\sigma_{eff}^n\cdot dt \tag{10}$$

where A, Q and n are coefficients that depend on temperature, strain rate and the α-β phase, which in turn depends on temperature and hydrogen content (Pastore et al., 2021).

Fig. 4 depicts the comparison between the Norton creep law and the MATPRO's correlation (Eq. (9)). As boundary conditions, a linear temperature rise from 300 °C to 1000 °C and a constant hoop stress of 50 MPa have been applied. The MATPRO's correlation has also been fed with null fast neutron fluence and cold work, that is to say, an unirradiated RXA Zircaloy cladding has been considered; furthermore, an

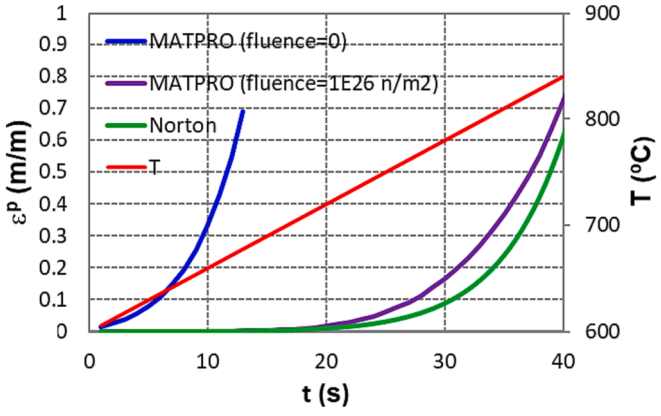

Fig. 4. Creep models comparison.

additional case with irradiated RXA Zircaloy has been included with a fast neutron fluence of 10^{26}n/m^2. As it can be observed from Fig. 4, there are huge differences between the estimations of the Norton creep law and the MATPRO's correlation for unirradiated cladding; particularly, the model from MATPRO predicts the highest deformation, although in case of the irradiated cladding the prediction gives rise to slightly higher deformation than the Norton creep law. This is due to the irradiation hardening effect included in the MATPRO's correlation, so that the higher the fast neutron fluence, the lower the estimated creep strain.

3.2. Bias

3.2.1. Creep model

The bias of the MATPRO's creep model (Eq. (9)) has been accounted for in this work through the information made available in USNRC (2001). Particularly, it has been implemented in FRAPTRAN the following bias concerning K, n and m parameters (called UK, Un and Um, respectively):

$$UK = \begin{cases} 77{\cdot}10^{6}\ ,\ T < 427\,^{\circ}C \\ 110.4{\cdot}10^{6} - 4.8{\cdot}10^{4}{\cdot}T\ ,\ 427 \leqslant T \leqslant 527\,^{\circ}C \\ K/3\ ,\ T > 527\,^{\circ}C \end{cases} \quad (11)$$

$$Un = \begin{cases} 0.017\ ,\ T < 427\,^{\circ}C \\ -2.8{\cdot}10^{-2} + 6.5{\cdot}10^{-5}{\cdot}T\ ,\ 427 \leqslant T \leqslant 982\,^{\circ}C \\ 0.053\ ,\ T > 982\,^{\circ}C \end{cases} \quad (12)$$

$$Um = \begin{cases} 0.01\ ,\ T < 427\,^{\circ}C \\ -2.98{\cdot}10^{-2} + 5.7{\cdot}10^{-5}{\cdot}T\ ,\ 427 \leqslant T \leqslant 627\,^{\circ}C \\ 0.16{\cdot}m\ ,\ T > 627\,^{\circ}C \end{cases} \quad (13)$$

It should be noted that the parameters K, n and m also affect the mechanical calculations in FRACAS-I, so the corresponding bias will also have an impact in the small deformations estimated by the code.

Regarding the bias of the Norton creep law (Eq. (10)), it has been estimated from the supporting database, gathered from Rosinger et al. (1979). Fig. 5 shows a non-negligible scatter of the model with respect to the data. Based on that, the standard deviation has been derived, from which the bias of the creep law has been expressed as follows:

$$\begin{aligned} \dot{\varepsilon}^{p+} &= \dot{\varepsilon}^{p}{\cdot}(1 + cf{\cdot}rstd) \\ \dot{\varepsilon}^{p-} &= \dot{\varepsilon}^{p}/(1 - cf{\cdot}rstd) \end{aligned} \quad (14)$$

where $\dot{\varepsilon}^{p+}$ and $\dot{\varepsilon}^{p-}$ are the upper and lower bounds of the creep rate, respectively, rstd is the relative standard deviation (a value of 3.01 is estimated) and cf is the coverage factor. In Fig. 5, the dashed lines represent the bias with a cf of 1 (68 % of the scattering is covered).

Fig. 6 represents the comparison between the MATPRO's correlation and the Norton creep law, taking into account the bias of both. The boundary conditions applied are the same as in the previous section. It should be noted that the bias cannot fully explain the differences previously observed between the models with a null fast neutron fluence; instead, in the case with irradiated cladding the MATPRO's law bias is very large and it encompasses the Norton law bias.

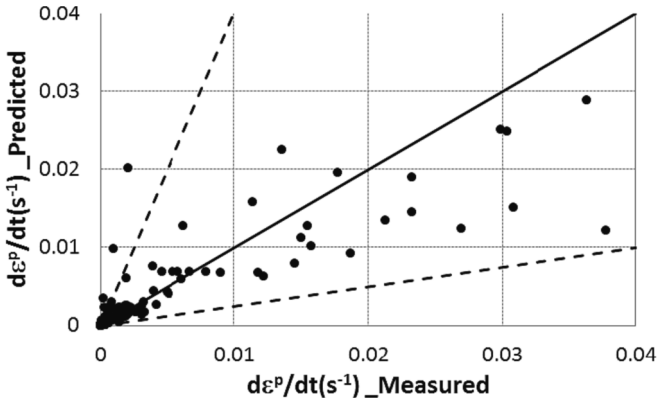

Fig. 5. Model-to-data comparison of the Norton creep law.

3.2.2. Failure limits

The bias of the stress and strain limits used by BALON2 for cladding failure in FRAPTRAN has been derived from the scattering of the supporting database, shown in Geelhood at al. (2016). Fig. 7 shows the comparison of the empirical limits with the data. It can be observed an important scattering, being especially relevant in the cladding strain. Based on that, the bias has been implemented in the code through multiplying factors that allow covering the dispersion found (dashed lines in Fig. 7). Table 1 shows the values applied for the upper and lower bounds.

4. Assessment

The FRAPTRAN's mechanical predictability under LOCA conditions has been tested using both models biases and new implementations, as described in the previous sections. It has been used the last version of FRAPTRAN (2.0) and in case of simulation with previous irradiation, FRAPCON-4.0 is used for the steady-state calculations.

The assessment has been done with two kinds of tests: out-of-pile and in-pile. For each test, the following cases have been simulated:

- Best estimate with MATPRO's correlation for creep (BE).
- Estimation with MATPRO's correlation for creep plus bias of K, n, m parameters and failure limits (BE + BIAS).
- Best estimate with Norton creep law (BE*).
- Estimation with Norton creep law plus bias of K, n, m parameters, creep and failure limits (BE*+BIAS).

Additionally, simulations without the bias of the failure limits have been carried out to check their impact (called BE + BIASwoLim. and BE*+BIASwoLim.). Note that in the figures shown in the following sections, in the cases simulated with bias, the bound closer to the experimental data is represented.

4.1. Out-of-pile

The tests selected in this case come from the PUZRY series (burst tests) with PWR Zr-4 tubes. Each test entailed a linear operator-defined pressure ramp under isothermal conditions (details shown in Perez-Feró et al., 2010). In this work, six PURZY tests have been simulated with FRAPTRAN by imposing the boundary conditions shown in Table 2.

Fig. 8 depicts the error obtained in the time to failure of each test simulated with the different options implemented in FRAPTRAN (refer to values in Table 3). In all the cases, there is a non-negligible underprediction of the best estimate with FRAPTRAN by default (i.e., simulation with MATPRO's creep model), even if the bias is included. This error is shown to be reduced with the Norton creep law, giving rise to overpredictions at temperatures above 900 °C, which can be explained with the corresponding bias (i.e. the resultant uncertainty covers the error). At 900 °C, the error from the underprediction obtained is also covered with the upper bound from the simulation with bias. At temperatures below, it seems that the higher pressurization rates prevent from being more accurate even with the bias. Based on these results, the code modifications with the Norton law, although they seem to offer a promising alternative option to the one by default, still require further improvement.

In order to perform a deeper analysis of the prediction of key variables in the cladding mechanical performance up to the failure, the PUZRY-8 test has been selected. Fig. 9 represents the overpressure increase up to burst both measured and predicted. As it can be observed, the bias of K, n and m allows reducing the error obtained with the best

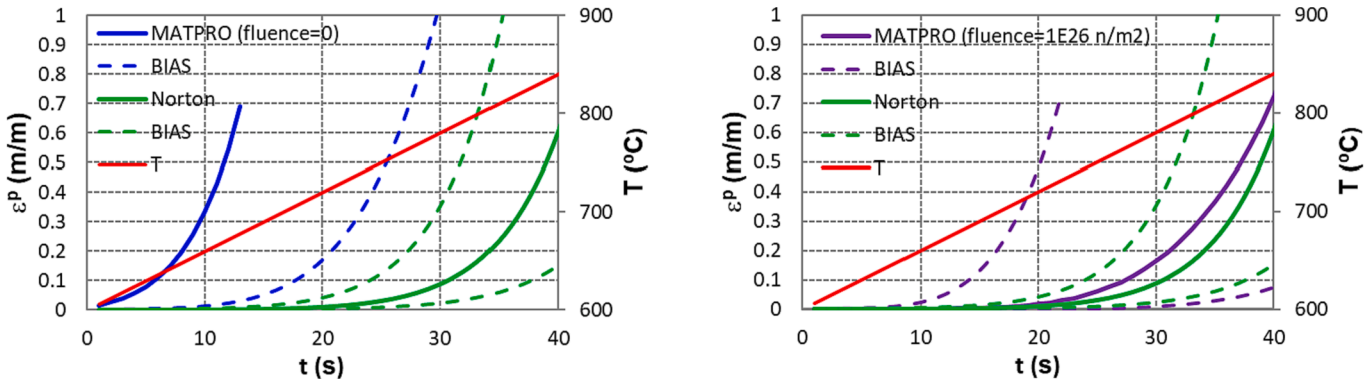

Fig. 6. Creep models comparison, bias included, for unirradiated cladding (Figure on the left) and irradiated cladding (Figure on the right).

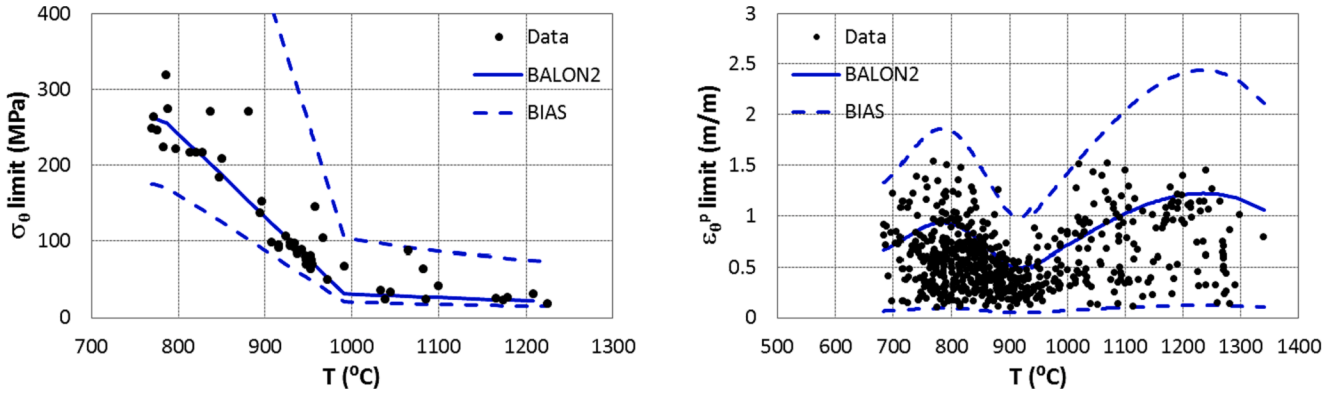

Fig. 7. Comparison of the cladding failure limits with data: true hoop stress limit (Figure on the left) and plastic hoop strain limit (Figure on the right). Bias included (dashed lines).

Table 1
Factor of limits bias.

Limit	Upper bound	Lower bound
Strain	2	0.1
Stress	3.3	0.7

Table 2
PUZRY tests.

PUZRY	Temperature (°C)	Pressure rate (bar/s)
26	700	0.119
30	800	0.2663
18	900	0.115
8	1000	0.076
10	1100	0.071
12	1200	0.072

estimate of FRAPTRAN by default, although it is not enough to explain the early burst predicted, as previously mentioned. The simulation with the alternative creep modelling (Norton law) gives rise to a prediction closer to the data if the corresponding bias is accounted for (as mentioned above, the bound closer to the experimental data is represented); indeed, an important impact of the creep model on the time to failure predicted is observed. On the contrary, the bias of the failure limits does not show any impact on the prediction. Similar outcomes have been derived from the other tests simulated.

In order to better understand the results obtained with the overpressure increase, an analysis of the cladding strain and stress has been done. First, the FRAPTRAN's results with the MATPRO's creep model have been studied (Fig. 10). The following observations should be highlighted:

- Discontinuity in the estimation of the cladding permanent hoop strain from 5 % to around 10 % when switching between FRACAS-I and BALON2. This was also observed in previous works with FRAPTRAN (e.g., see Fig. 20 in He et al., (2019)). It is related to the initialization of the strain components in BALON2, which does not directly come from the previous strain calculation in FRACAS-I (based on constitutive laws of strain vs stress); instead, the initial strain in BALON2 is calculated from the cladding geometry (i.e., radius) at the end of the pre-ballooning phase.
- Failure is due to overstrain, except when the strain limit is biased, which gives rise to failure due to the overstress.
- The sharpen increase of the strain and stress close to the time to failure prevents from any effect of the bias of the failure limits.
- The lower strain related to the K, n and m bias allows delaying the ballooning and, as a consequence, the time to failure. In fact, the impact of this bias on the small deformations is the main contribution for the resultant delay in the time to failure. Minor impact of this bias is observed during ballooning.

Finally, in order to analyse the effect of the creep model on the cladding strain, Fig. 11 depicts the results obtained with the best estimate of both the MATPRO's correlation and the Norton law. The Figure shows how the lower deformation of the Norton law during ballooning gives rise to a strong impact in the delay of the time to failure (stronger than the impact of the bias of K, n and m).

4.2. In-pile

In order to simulate an irradiated fuel rod under LOCA conditions,

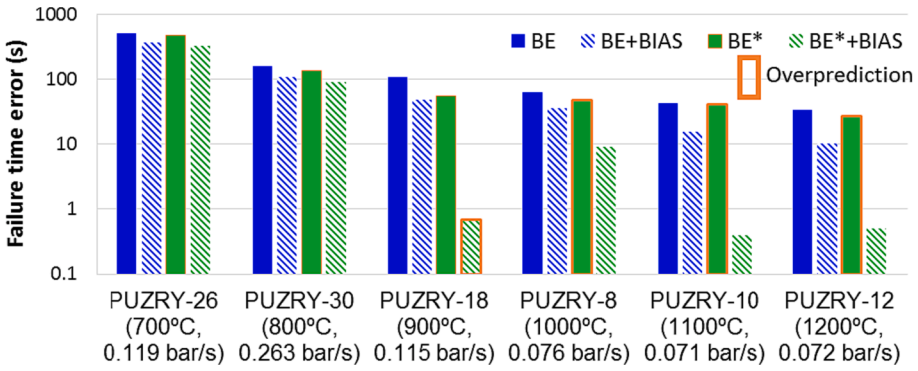

Fig. 8. Model-to-data comparison for the time to failure of PUZRY tests. Cases with overprediction highlighted in orange.

Table 3
Time-to-failure errors in PUZRY tests simulations.

PUZRY	BE (s)	BE + BIAS (s)	BE* (s)	BE*+BIAS (s)
26	520.2	374.7	479.2	331.7
30	160	110	134	91.5
18	107.3	49.3	54.8	−0.7
8	63.3	36.8	−47.2	9.3
10	43.4	15.9	−41.1	0.4
12	34	10.5	−27	0.5

the IFA-650.10 test has been selected as a representative scenario. It comes from the Halden research reactor that operated under the framework of the OECD-NEA Halden Reactor Project. Particularly, the test simulated belongs to one of its experimental series, IFA-650, that was specifically aimed at testing fuel rodlets under LOCA conditions (Lavoil, 2010).

The IFA-650.10 test was preceded by a steady state irradiation. Particularly, the mother rod is a standard PWR fuel rod (Zircaloy-4 cladding and UO_2 fuel) irradiated in Gravelines 5 (900 MWe) to an average burnup of 61 GWd/tU. Then, the mother rod was refabricated into the test rodlet (440 mm segment), which was surrounded by an electrical heater and placed in a high-pressure flask. This device contained instrumentation for measuring rod internal pressure among other relevant variables. A description of the mother rod irradiation, the rodlet tested and the experimental device is given elsewhere (Nishi and Lee, 2001; Lavoil, 2010).

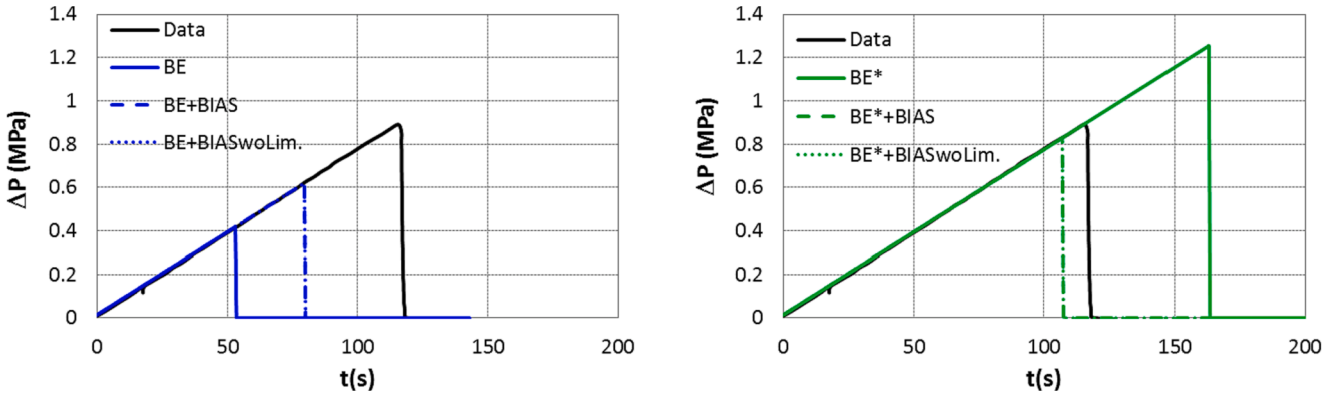

Fig. 9. Model-to-data comparison for the overpressure (ΔP) increase in PUZRY-8. Predictions with MATPRO's creep model on the left and with Norton law on the right.

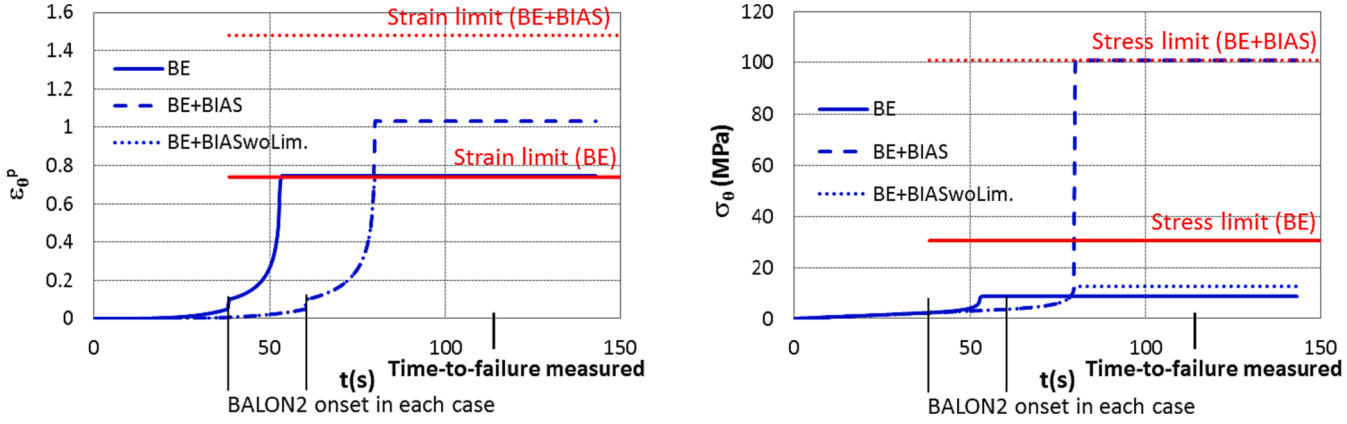

Fig. 10. Predictions in PUZRY-8 with MATPRO's creep model. Cladding plastic hoop strain on the left and hoop stress on the right.

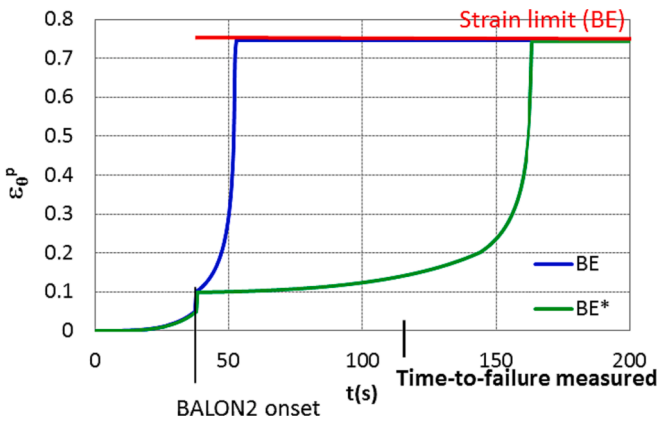

Fig. 11. Predictions of cladding plastic strain in PUZRY-8 with MATPRO's and Norton creep models.

The simulation of the LOCA test with FRAPTRAN has been fed with the irradiation conditions of the mother rod, simulated with the steady state fuel performance code FRAPCON, as well as transient thermal conditions specified, both detailed in Vallejo and Herranz (2014) and Herranz and Peláez (2016).

Fig. 12 shows the results obtained in terms of the rod internal pressure evolution. The main observations are the following:

- The best estimate simulation with the MATPRO's creep model (estimation by default) gives rise to early time to failure (i.e., underprediction with respect to the measurement), as in the out-of-pile tests.
- An accurate estimation of the upper bound corresponding to the bias of K, n and m parameters is obtained. In other words, the model bias may to some extend explain the error found with the best estimate. The main contribution to the upper bound corresponding uncertainty is related to the small deformation region (before ballooning), as in the out-of-pile tests.
- As expected from the discussions in the previous section, the bias of the failure limits does not impact to the prediction of the time to failure.
- The estimation with the Norton creep law does not improve the accuracy of the estimation by default, not even with the bias of K, n, m parameters and creep. A possible explanation might be that the Norton creep law does not include the irradiation hardening effect, which would lead to smaller strains and thus delay the time to failure (note that under the test conditions the code predicts a non-full recovery of the irradiation hardening resulting from the base irradiation).

Fig. 13 represents the cladding strain and stress evolution for the best estimate with the MATPRO's creep model. At the BALON2 onset it is observed the same strain discontinuity previously explained in Fig. 10. As it can be seen, the failure is due to stress, which fast increase close to the time to failure make the effect of the failure limits bias be minor. Instead, the lower strain obtained with the bias of K, n and m parameters allows delaying the ballooning and, as a consequence, the time to failure (in accordance with the out-of-pile tests results). From Fig. 14 it can be deduced that the higher deformation from the Norton creep law enlarges the time-to-failure error with respect to the estimation with the MATPRO's model (irradiation hardening effect included).

5. Conclusions

The evaluation of the cladding mechanical model of the FRAPTRAN's code under LOCA conditions has been carried out in this work. The study has been focused on the cladding burst due to ballooning based on the simulation of burst (out-of-pile) and LOCA (in-pile) tests. This has been done with the code by default and with a code extension that takes into account the bias of the creep model and the failure limits, as well as an alternative creep model (Norton law).

The assessment performed allows confirming that FRAPTRAN by default gives rise to conservative results of the time to failure, which is on the safety side. However, depending on the boundary conditions, an important underprediction may be obtained.

Based on the application of the code extended, it is concluded that the enhancement of the FRAPTRAN accuracy in the time-to-failure prediction goes through properly modelling the viscoplastic performance of the cladding (i.e., creep). The Norton-type creep law could be an alternative formulation to enhance the code accuracy but, given that it does not notably enhance the prediction by default, it should be further studied; particularly, the irradiation hardening effect should be considered (in case there is not full annealing). On the contrary, the accuracy enhancement cannot be achieved through the failure limits. Additionally, the results obtained allows concluding that the plastic strain modelling up to the instability strain also plays an important role in the prediction of the failure.

From the results obtained further work is foreseen to enhance the code estimation of the cladding large deformation at high temperature on the basis of the Norton creep law; its extension to the irradiation hardening effect would depend on the data made available from irradiated claddings under LOCA conditions.

CRediT authorship contribution statement

F. Feria: Conceptualization, Investigation, Methodology, Software, Writing – original draft. **P. Aragón:** Investigation, Methodology, Software, Writing – original draft. **L.E. Herranz:** Investigation, Writing – review & editing.

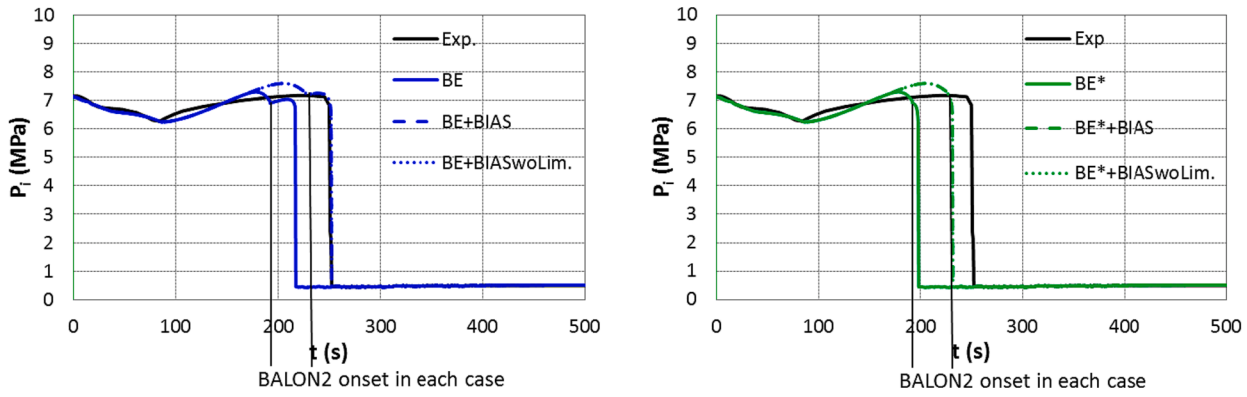

Fig. 12. Model-to-data comparison for the internal pressure (P_i) in IFA-650.10. Predictions with MATPRO's creep model on the left and with Norton law on the right.

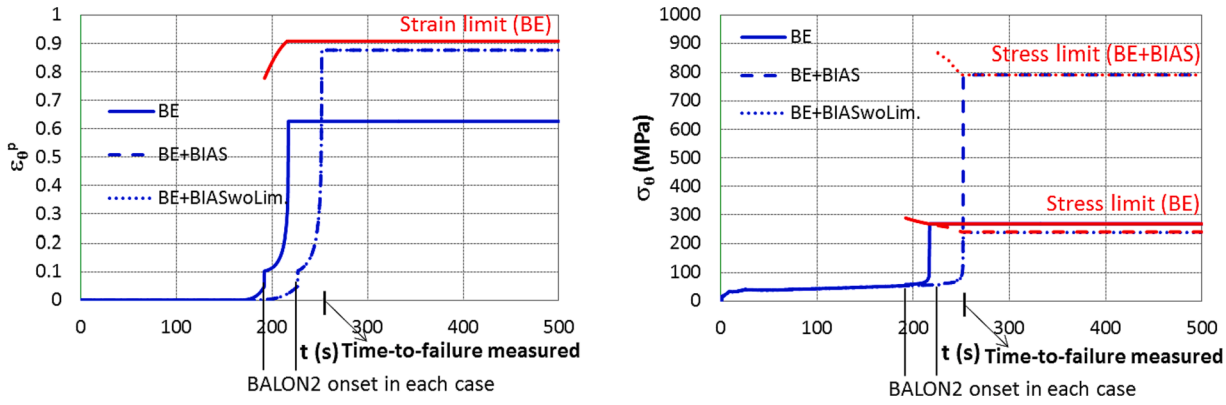

Fig. 13. Predictions in IFA-650.10 with MATPRO's creep model. Cladding plastic hoop strain on the left and hoop stress on the right.

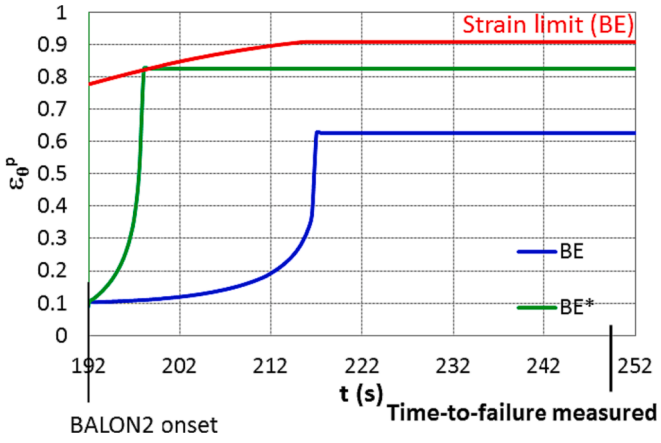

Fig. 14. Predictions of cladding plastic strain in IFA-650.10 with MATPRO's and Norton creep models (BE does not reach the strain limit because the failure is due to stress in this case; see Fig. 12).

Declaration of Competing Interest

The authors declare that they have no known competing financial interests or personal relationships that could have appeared to influence the work reported in this paper.

Data availability

The authors do not have permission to share data.

Acknowledgment

The authors wish to thank the funding from the MATMEC and R2CA projects. The former is a project from the Spanish Nuclear Safety Council and the latter comes from the Euratom research and training programme 2014-2018 under grant agreement No 847656.

Views and opinions expressed in this paper reflect only the authors' view and the European Commission is not responsible for any use that may be made of the information it contains.

References

Di Marcello, V., Schubert, A., van de Laar, J., Van Uffelen, P., 2014. The TRANSURANUS mechanical model for large strain analysis. Nucl. Eng. Des. 276, 19–29.

Geelhood, K.J., Beyer, C.E., Luscher, W.G., 2008. PNNL Stress/Strain Correlation for Zircaloy. PNNL-17700.

Geelhood, K.J., Luscher, W.G., Cuta, J.M., Porter, I.A., 2016. FRAPTRAN-2.0: A Computer Code for the Transient Analysis of Oxide Fuel Rods. PNNL-19400 Vol. 1 Rev2.

Hagrman, D.L., 1981. Zircaloy cladding shape at failure (BALON2). EGG-CDAP-5379.

He, Y., Shirvan, K., Wua, Y., Su, G., 2019. Integrating a multi-layer deformation model in FRAPTRAN for accident Tolerant fuel analysis. Ann. Nucl. Energy 133, 441–454.

Herranz, L.E., Peláez, S.B., 2016. Assessment of FRAPTRAN-1.5 Capabilities for Clad-to-Coolant Heat Transfer under Loss of Coolant Accidents. Enlarged Halden Programme Group Meeting, Fornebu, Norway.

IAEA, 2012. Fuel Modelling at Extended Burnup (FUMEX-II). IAEA TECDOC-1687.

IAEA, 2013. Improvement of computer codes used for fuel behaviour simulation (FUMEX-III). IAEA-TECDOC-1697.

IAEA, 2019. Fuel Modelling in Accident Conditions (FUMAC). IAEA-TECDOC-1889.

IAEA, 2020. Modelling of Fuel Behavior in Design Basis Accidents and Design Extension Conditions. IAEA-TECDOC-1913.

Karb, E.H., Pruessmann, M., Sepold, L., Hofmann, P., Schanz, G., 1983. LWR fuel rod behavior in the FR2 in-pile tests simulating the heatup phase of a LOCA. Final report. KFK-3346.

Lavoil, A., 2010. LOCA testing at Halden, the tenth experiment IFA-650.10. HWR-974, OECD Halden Reactor Project.

Meyer, R.O., Wiesenack, W., 2022. A critique of fuel behavior in LOCA safety analyses and a proposed alternative. Nucl. Eng. Des. 394, 111816.

Nishi, N., Lee, B.H., 2001. Summary of pre-irradiation data on fuel segments supplied by EDF/FRAMATOME and tested in IFA-610, 629 and 648. HWR-664, OECD Halden Reactor Project.

OECD/NEA, 2016. Report on Fuel Fragmentation, Relocation and Dispersal. NEA/CSNI/R(2016)16.

Pastore, G., Williamson, R.L., Gardner, R.J., Novascone, S.R., Tompkins, J.B., Gamble, K. A., Hales, J.D., 2021. Analysis of fuel rod behavior during loss-of-coolant accidents using the BISON code: Cladding modeling developments and simulation of separate-effects experiments. J. Nucl. Mater. 543, 152537.

Peláez and Herranz, 2017. Assessment of FRAPTRAN modeling of large strains under loss of coolant accidents. Water Reactor Fuel Performance Meeting.

Perez-Feró, E., Győri, C., Matus, L., Vasáros, L., Hózer, Z., Windberg, P., Maróti, L., Horváth, M., Nagy, I., Pintér-Csordás, A., Novotny, T., 2010. Experimental database of E110 claddings exposed to accident conditions. J. Nucl. Mater. 397 (1-3), 48–54.

Rosinger, H.E., Bera, P.C., Clendening, W.R., 1979. Steady-state creep of Zircaloy-4 fuel cladding from 940 to 1873 K. J. Nucl. Mater. 82 (2), 286–297.

Stuckert, J., Grosse, M., Steinbrueck, M., Walter, M., Wensauer, A., 2020. Results of the QUENCH-LOCA experimental program at KIT. J. Nucl. Mater. 534, 152143.

USNRC, 2001. SCDAP/RELAP5/MOD 3.3 Code Manual MATPRO - A Library of Materials Properties for Light-Water-Reactor Accident Analysis. NUREG/CR-6150, Vol. 4, Rev. 2.

USNRC, 2021. General Design Criteria for Nuclear Power Plants. U.S. Code of Federal Regulations, Part 50, Appendix A.

Vallejo, I., Herranz, L. E., 2014. HALDEN LOCA tests: Simulations of IFA-650.3, .5 and .10 with FRAP Serie Codes. Preliminary Results and Comparisons to Experimental Data", Enlarged Halden Programme Group Meeting, Røros, Norway.

Wiesenack, W., 2013. Summary of the Halden Reactor Project LOCA Test Series IFA-650. HPR-380 (May 14, 2013).

Wiesenack, W., 2015. Summary and Comparison of LOCA Tests with BWR Fuel in the Halden Reactor Project Test Series IFA-650. HPR-383 (June 30, 2015).